View Article Online / Journal Homepage / Table of Contents for this issue

PAPER

NJC
www.rsc.org/njc

Selective control of cubic and hexagonal mesophases for titania and silica thin films with spin-coating

Jia Hong Pan[ab] and Wan In Lee*[a]

[a] *Department of Chemistry, Inha University, 402-751 Incheon, Korea. E-mail: wanin@inha.ac.kr; Fax: +82-32-867-5604; Tel: +82-32-863-1026*
[b] *Department of Chemistry, Xiamen University, Xiamen, 361005, P. R. China*

Received (in Montpellier, France) 12th November 2004, Accepted 11th March 2005
First published as an Advance Article on the web 5th May 2005

Downloaded by University of California - Los Angeles on 01 January 2013
Published on 05 May 2005 on http://pubs.rsc.org | doi:10.1039/B417310D

Highly organized mesoporous titania and silica thin films were synthesized using a triblock copolymer-templated sol-gel method *via* an evaporation-induced self-assembly (EISA) process. For the first time, we have found that the mesophase of these metal oxides can be selectively controlled by varying the spin-coating conditions. With spin-coating at a low speed, such as 600 rpm, cubic mesoporous TiO_2 or SiO_2 thin films are obtained, whereas 2D hexagonal mesoporous thin films are formed at a high spin-coating speed of around 2000 rpm for 20 s. On the other hand, a mixture of hexagonal and cubic phase is formed for films prepared at an intermediate spinning speed of 1000 rpm for 10 s. The fabricated mesoporous thin films, characterized by XRD, TEM, and UV-visible spectroscopy, show that the mesopore structures are highly ordered, without any cracks, and thermally stable (up to 400 °C). The hexagonal and cubic mesoporous TiO_2 films of 300–320 nm thickness have about 95% transparency and exhibit a ultra-uniform surfaces. We believe that the evaporation rate of volatile components in the coated film is qualitatively proportional to the speed of spin-coating, and this determines the mesophase of the resultant films.

Introduction

Since the discovery of the MCM family, mesoporous materials derived from the supramolecule-templated sol-gel method have attracted great interest from scientific and industrial societies. In the presence of ionic or non-ionic surfactants, including quaternary ammonium salts or block copolymers, as structure-directing agents, mesoporous materials with various mesophases and pore sizes have been synthesized in the form of powders, films, monoliths, fibers, *etc*.[1–6] Considerable efforts have been extended to other metal oxides because of their potential applications, after the discovery of mesoporous silica-based molecular sieves. However, due to the high reactivity of metallorganic precursors, and the easy collapse of mesoporous inorganic frameworks during crystal phase transform and grain growth upon calcination, the efficient synthesis of mesoporous transition metal oxides with highly ordered mesostructures and their thermal stability still remain a challenge.[7–9]

In preparing mesoporous metal oxides, amphiphilic block copolymers, providing a robust wall structure and high synthetic reproducibility, are considered to be among the most promising templates.[10–12] In order to control the hydrolysis and condensation of inorganic sources, including metal alkoxides and chlorides, a non-aqueous medium is essential.[8,9,12] Thus, the so-called evaporation-induced self-assembly (EISA) process, initiated by Brinker's group, has allowed the facile fabrication of mesoporous materials, especially for thin films.[13,14] As the solvent evaporates, the concentration of surfactant in the sol solution begins to exceed the critical micelle concentration, and the self-assembly procedure is triggered at the same time.[13–17]

TiO_2 has been extensively investigated in diverse applications, such as photocatalysts,[18] electrochromic devices,[19,20] photovoltaics,[21–23] host-guest chemistry,[24,25] luminescent devices,[26] *etc*. The tailoring of highly ordered mesoporous structures of TiO_2 thin films is of great importance for the realization of these applications. In general, the hexagonal or cubic mesophases can be predicted by adjusting the template volume fraction (Φ_T). Alberius *et al*. reported that cubic mesoporous SiO_2 and TiO_2 films were formed with a low P123 concentration, whereas the hexagonal phase was obtained with a relatively high P123 concentration.[27] However, the hexagonal mesoporous TiO_2 thin films showed lower thermal stability with a comparatively high surfactant incorporation. Bosc *et al*. also reported that the cubic and hexagonal mesophases of TiO_2 thin films can be controlled by varying the nature of the triblock copolymer.[28] Similar results were also observed for mesoporous SiO_2 thin films.[29] Sanchez's group has systematically studied mesophase control of TiO_2 thin films.[30–34] A set of aging steps between the deposition and calcination was introduced to stabilize and to control the mesostructures. In their process, the final regularity and mesophase of the dip-coated films were critically determined not only by the initial sol conditions (template type, Φ_T, water content, pH value, *etc*.) and the ramping rate of the thermal treatment, but also by the aging procedure (aging time, atmospheric conditions, relative humidity (RH) value, *etc*.). They also extended this EISA method to the formation of mesoporous films of various metal oxides, such as ZrO_2,[34,35] Al_2O_3,[36] and several mixed oxides.[37–39] Cubic mesoporous films were generally formed with aging under a high RH, while the hexagonal mesophase was obtained under a low RH.

So far, most mesoporous TiO_2 films have been prepared by the dip-coating method. Only a few groups have reported the preparation of mesoporous TiO_2 films with the spin-coating method, and all of their prepared thin films were 2D-hexagonal mesostructures, whose pore channel is parallel to the surface of the substrate.[20,22,40–43]

In this work, we report that the spin-coating conditions during the EISA process can also influence the mesopore structures of TiO_2 and SiO_2 films. That is, hexagonal and cubic mesophases have been selectively controlled by varying the spin-coating speed.

DOI: 10.1039/b417310d

View Article Online

Results and discussion

We chose a comparatively solvent-rich Ti-sol for the preparation of mesoporous TiO_2 films, since the spin-coating method is considered to be a fast evaporation process compared with the dip-coating method. For the same reason, the coated films were aged under a relatively high humidity atmosphere. Hence, the molar composition ratio TTIP : F127 : HCl : H_2O : EtOH was adjusted to 1 : 0.005 : 1.75 : 10 : 25. The prepared Ti sol solution was spin-coated at 600 rpm for 5–20 s, and aged under moist conditions for 3 days. The optimum RH for the aging was 55–70%. Then, it was heat-treated at 150, 250, 350, and 400 °C under ambient conditions for 4 h.

The XRD patterns in Fig. 1 indicate that the prepared films have a highly ordered cubic structure. The films annealed at 150 °C show only (200) and (400) reflection peaks, but the films annealed at 250 °C show (100), (110), (200), (211), (220) and (400) peaks. From the thermal gravimetric analysis it is found that most of the volatile component is evaporated below 150 °C, while the triblock copolymer used for the liquid-crystal template is removed at 250–350 °C. Thus, it is deduced that ordering of the mesoporous structure is still going on even after complete evaporation of solvent above 150 °C. From the first three peaks, assumed to be (100), (110), and (200), the *d* value ratio was determined to $1 : 1/\sqrt{2} : 1/2$. Therefore, the position of the (110) peak is clear evidence for the formation of a cubic mesophase. Even the films annealed at 400 °C show (100), (110), (200), and (400) peaks, suggesting that the cubic mesophase is retained at least up to 400 °C. As far as we know, this is one of the best results so far reported.[18,27,34,40,41] For the films annealed at 150 °C, the *d*(100) spacing was calculated to 16.2 nm. However, that of the films annealed at 250, 350, and 400 °C was 10.64, 10.12, and 9.86 nm, respectively. This indicates that most of the shrinkage in this mesoporous TiO_2 structure occurs at 150–250 °C and the shrinkage is virtually completed at around 350 °C.

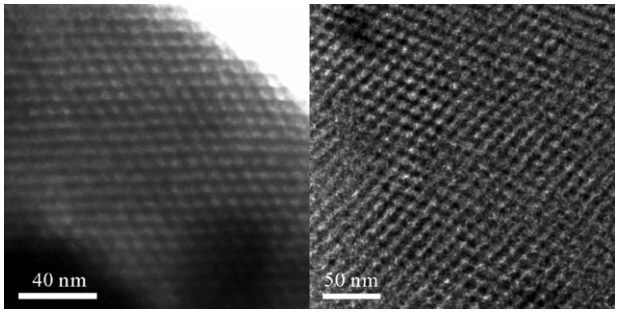

Fig. 2 TEM micrographs for the cubic mesoporous TiO_2 films spin-coated at 600 rpm for 5 s, then calcined at (a) 350 and (b) 400 °C.

Plane-view TEM images in Fig. 2 show (100) oriented cubic mesoporous TiO_2 films annealed at 350 and 400 °C. The mesopores for both films are regularly ordered, and the *d*(100) for the mesostructure annealed at 400 °C is estimated to about 10 nm, which is consistent with the result obtained from the XRD pattern.

The Ti-sol of the same composition was used for the preparation of hexagonal mesoporous TiO_2 films. After spin-coating, the film was aged under moist conditions (RH = 60%) for 3 days, then heat-treated at 150–400 °C. The only the difference in this preparation procedure was the speed of spin-coating. That is, the Ti-sol was spin-coated at 2000 rpm on a Pyrex glass substrate. The resultant TiO_2 film exhibits a highly ordered hexagonal mesoporous structure, as indicated by the X-ray diffraction patterns in Fig. 3. For the films annealed at 150 and 250 °C, the (210) peak appears in addition to the (*n*00) peaks. The position of the (210) peak is clear evidence for the presence of the hexagonal mesoporous structure. However, the

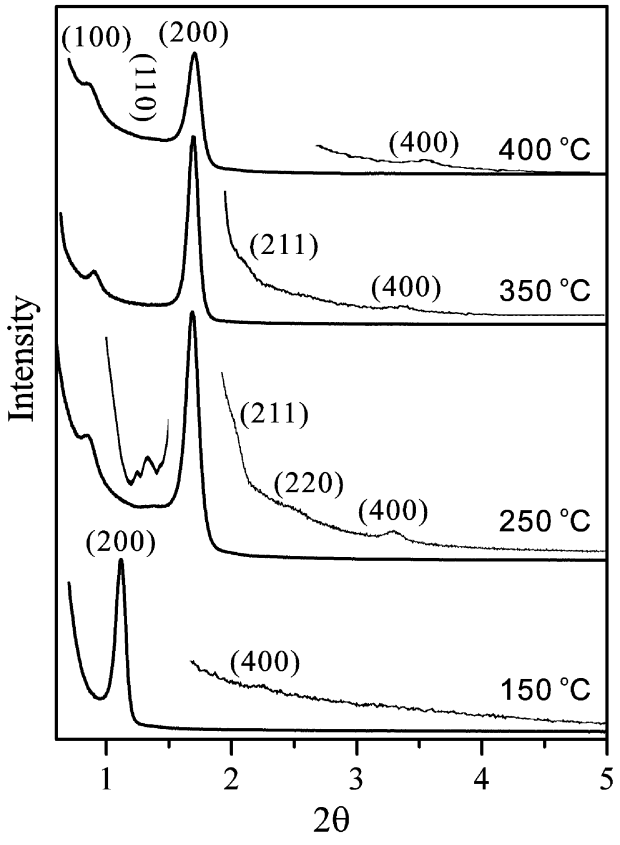

Fig. 1 Small-angle X-ray diffraction patterns for cubic mesoporous TiO_2 thin films spin-coated at 600 rpm for 5 s, then calcined at several temperatures. In the initial Ti-sol, the molar ratio of TTIP : F127 : HCl : H_2O : EtOH = 1 : 0.005 : 1.75 : 10 : 25.

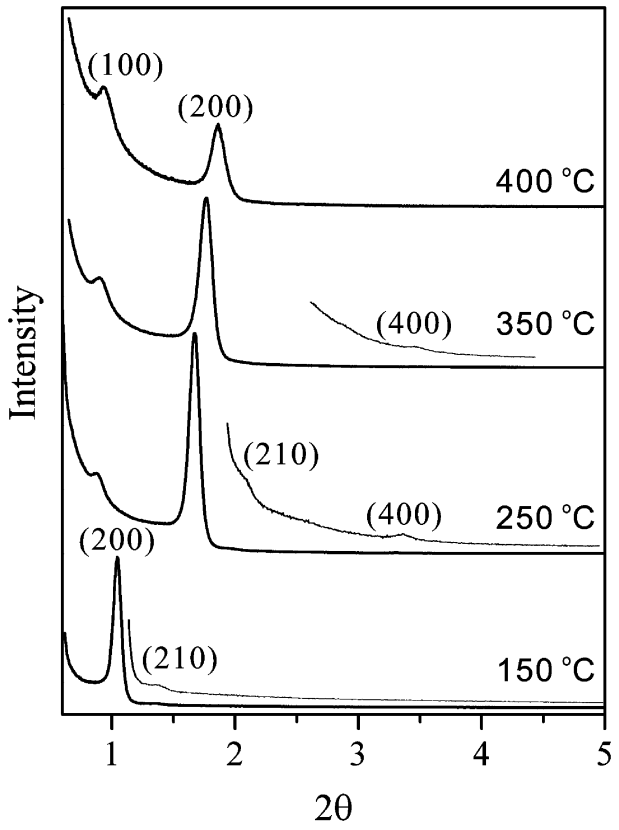

Fig. 3 Small-angle X-ray diffraction patterns for hexagonal mesoporous TiO_2 thin films spin-coated at 2000 rpm for 20 s, then calcined at several temperatures.

Published on 05 May 2005 on http://pubs.rsc.org | doi:10.1039/B417310D
Downloaded by University of California - Los Angeles on 01 January 2013

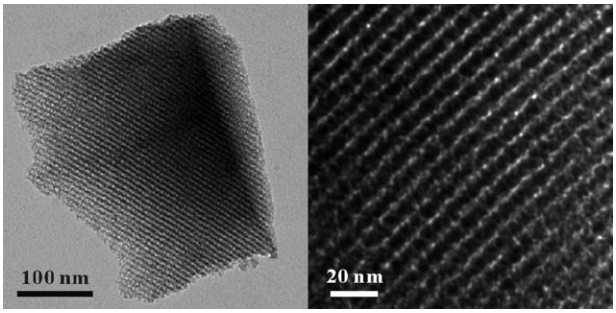

Fig. 4 TEM micrographs for the hexagonal TiO_2 thin films prepared by spin-coating at 2000 rpm for 20 s, then annealing at 400 °C.

films annealed at 400 °C show only the (*n*00) plane peaks. This suggests that the hexagonal mesoporous channels initially formed at low temperature are aligned in a 3-dimensional way, but this random array is gradually changed to a 2-dimensional array with elevation of the calcination temperature. For the films annealed at 150 °C, the *d*(100) spacing was determined to be 16.9 nm. With increase of the annealing temperature to 250, 350 and 400 °C, the *d*(100) spacings decreased to 10.6, 10.0, and 9.2 nm, respectively. The shrinkage of the cell parameters for the hexagonal mesoporous structure mostly occurred at 150–250 °C, with removal of surfactant, but still proceeded continuously up to 400 °C, whereas the shrinkage of the cubic mesoporous structure was almost completed at 350 °C (*vide supra*).

Plane-view TEM images in Fig. 4 show the hexagonally ordered mesoporous structures for TiO_2 films spin-coated at 2000 rpm for 20 s and subsequently annealed at 400 °C. The mesopore channels are straight and regularly arrayed parallel to the Pyrex substrate. The wall-to-wall distance was estimated to 9 nm, which is consistent with the cell parameter obtained from the XRD pattern.

Our observations so far are that a highly ordered cubic mesophase can be formed by spin-coating at 600 rpm for 5 s, whereas a hexagonal mesophase is formed by coating at 2000 rpm for 20 s. Then we have used spin-coating conditions between these two. That is, the same Ti-sol solution was spin-coated at 1000 rpm for 10 s, aged and heat-treated under the same conditions applied for the preparation of cubic or hexagonal mesoporous TiO_2 films. Fig. 5 shows a plane-view TEM image for the TiO_2 film coated at 1000 rpm and heat-treated at 350 °C. In the (110) oriented thin foil, a mixture of cubic and hexagonal mesoporous structures appears. Throughout the film, this combination of mesophases appears repeatedly, but a worm-like structure (or local cubic structure) is not at all observed.

Gibaud and Grosso *et al*. reported that the evaporation rate of the solvent during the aging step is one of the key parameters that determine the final mesophase of CTAB-templated SiO_2 thin films obtained by the dip-coating process.[17,44] They have indicated that the hexagonal mesostructure is relatively favorable under ethanol-deficient conditions. For the formation of the cubic mesophase, an ethanol-rich condition is necessary; it is subtly related to the competition between the evaporation rate of solvent, water diffusion, and the sol-gel reaction forming SiO_2. In our present work, with spin-coating at a low speed, an ethanol-rich condition can be obtained in the coated film. The extreme case would be a dip-coating process. Fig. 6 shows the TEM image and XRD patterns of a mesoporous TiO_2 thin film deposited by the dip-coating method. The film shows the same cubic mesostructure as the one prepared by low-speed spin-coating. In both cases, enough ethanol will remain in the as-coated films to decrease the Φ_T, which can lead to the formation of the cubic mesophase. However, XRD patterns in Fig. 6 indicate that the mesopore structure is not as well-organized as the one obtained by slow spin-coating.

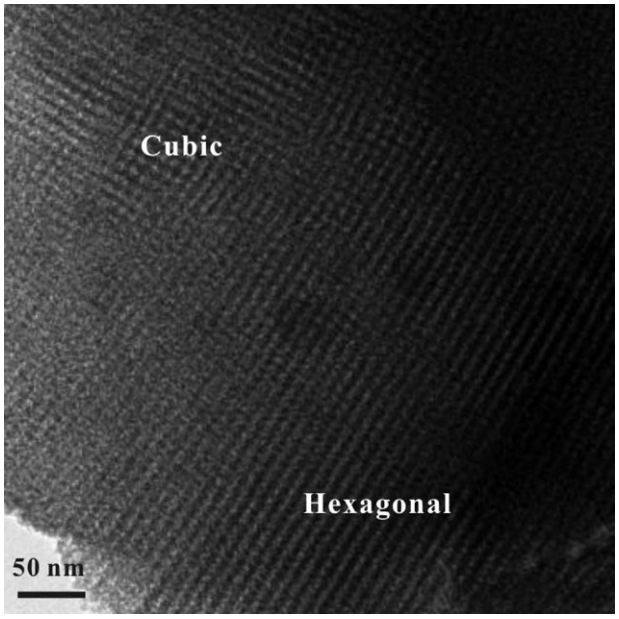

Fig. 5 TEM micrograph of the mesoporous TiO_2 thin films prepared by spin-coating at 1000 rpm for 10 s, then calcined at 350 °C.

The *d*(100) spacing of 9.18 nm, which is appreciably smaller than the slow spin-coating one, suggesting that the contraction of the mesostructure is more extensive for the dip-coated film.

In the spin-coating method, with the increase of spinning speed the volatile ethanol will be evaporated considerably faster than other components, such as water or acid. Thus, at high spinning rates an ethanol-deficient environment will be established in the spin-coated film, which can lead to the formation of the hexagonal phase. Presumably, the individual mesophase is already determined by the spin-coating conditions, even though the actual mesophase gradually evolves during the aging step with slow evaporation of solvent, re-orientation of surfactants and serial sol-gel reactions.

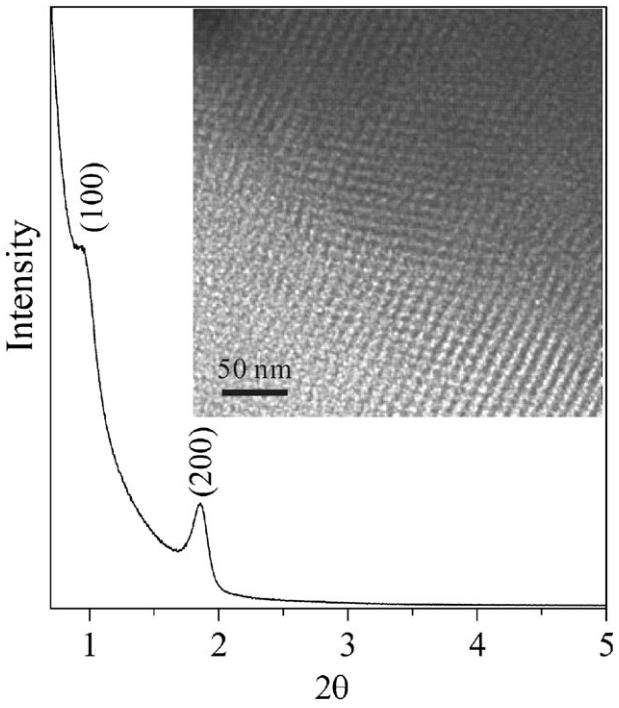

Fig. 6 Small-angle X-ray diffraction pattern and TEM micrograph (insert) for the mesoporous TiO_2 thin film deposited by the dip-coating process and calcined at 400 °C.

Downloaded by University of California - Los Angeles on 01 January 2013
Published on 05 May 2005 on http://pubs.rsc.org | doi:10.1039/B417310D

View Article Online

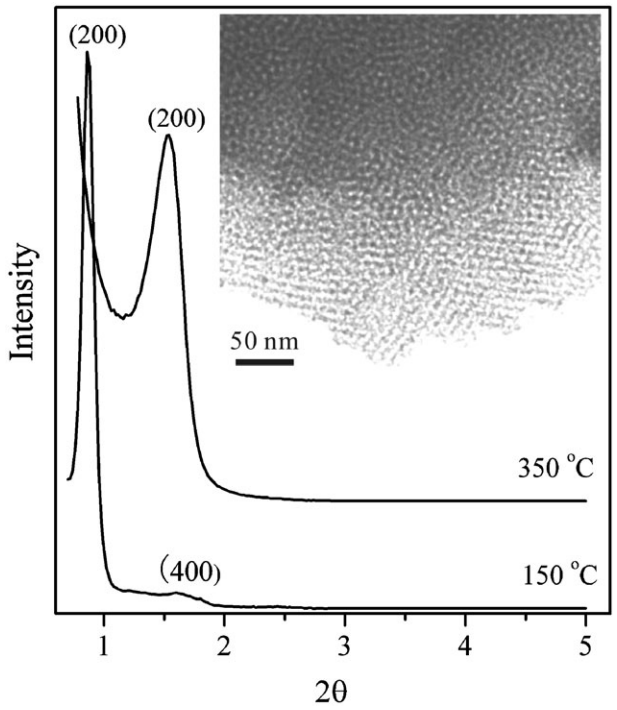

Fig. 7 Small-angle X-ray diffraction patterns and TEM micrograph (insert) for the mesoporous TiO_2 thin film derived from the Ti-sol with a relatively low solvent composition: molar ratio TTIP : F127 : HCl : H_2O : EtOH = 1 : 0.005 : 1.7 5 : 6 : 15. The prepared Ti-sol was spin-coated at 600 rpm, aged for 3 days at RH 60%, and subsequently annealed at 150 or 350 °C, respectively. The film shown in the TEM image was calcined at 350 °C.

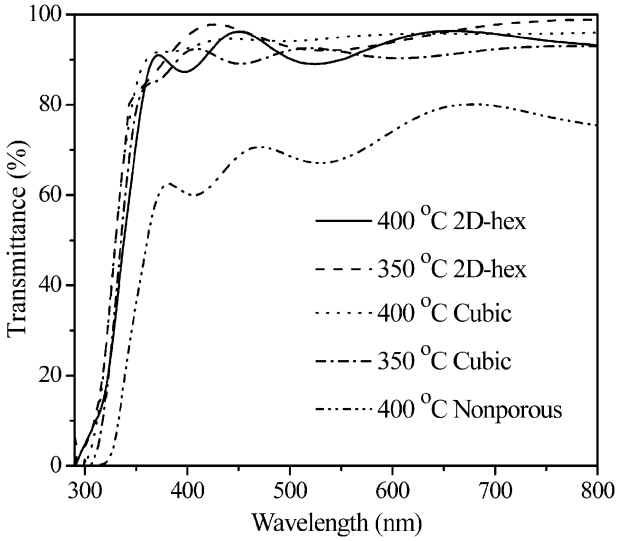

Fig. 8 UV-visible transmittance spectra for the cubic and hexagonal mesoporous TiO_2 films calcined at 350 or 400 °C, and for a nonporous, 320 nm thick, titania film prepared by the normal sol-gel process at 400 °C.

To investigate the effect of the spinning time, we varied it from 5 s to 20 s at each rpm during the spin-coating. The change of spinning time in this range did not alter the phase of the mesostructures, but it slightly influenced the degree of ordering. This indicates that the spinning time is a trivial factor in determining the mesophase of the TiO_2 films. The spinning times specified in this work are the optimized values in terms of the ordering of the mesostructures.

It is noteworthy that the worm-like mesostructure did not appear at all in any of the spin-coated mesoporous films. Even though the spinning speed was adjusted from zero to 3000 rpm, the worm-like mesoporous structure was never observed. In general, the worm-like mesostructure is formed when the inorganic polycondensation is faster than mesophase formation. In comparison, we applied a relatively solvent-deficient Ti-sol, which was suggested by Alberius *et al.*:[27] that is, TTIP : F127 : HCl : H_2O : EtOH was adjusted to 1 : 0.005 : 1.75 : 6 : 15. The spin-coating speed was 600 rpm and the subsequent aging and heat-treatment conditions were maintained exactly the same. Under these conditions the resultant TiO_2 films present only weak (200) peak as shown in the XRD patterns of Fig. 7, and a worm-like mesoporous structure was observed, as indicated by TEM image in its insert.

Since variation of the speed of spin-coating in the range 600–4000 rpm never produced the worm-like mesophase, and even the dip-coating process did not change the mesophase of the final TiO_2 film, this suggests that the final settlement to worm-like structure or long-range ordered mesoporous structure is already determined at the initial stage of the EISA process. If the worm-like structure is formed at an early stage, it may not be converted to long-range ordered structures.

On the other hand, under highly water-rich conditions, that is, when the molar composition ratio of TTIP : H_2O is increased to 1 : 20, the resultant films did not show any ordered mesoporous structure, regardless of the spin-coating speed. This may be due to quick hydrolysis of the titanium precursor in an early EISA process.

The thickness of the resultant TiO_2 films was not greatly dependent on the spinning speed because of the high viscosity of the initial sol. The hexagonal mesoporous TiO_2 thin film prepared by spin-coating at 2000 rpm was about 300 nm thick, while the cubic mesoporous film coated at 600 rpm was 320 nm thick. The surface of both films was very uniform and optically transparent. Fig. 8 shows the UV-visible spectra, demonstrating the transparency of the cubic and hexagonal mesoporous TiO_2 films. For comparison, a nonporous TiO_2 film of 320 nm thickness was fabricated by a simple sol-gel method with a Ti-sol prepared without addition of F127. The transmittance of mesoporous TiO_2 films, annealed at 350 or 400 °C, was about 95%, whereas that of the sol-gel derived nonporous TiO_2 film annealed at 400 °C was only 60–75%. It is concluded that the high transmittance of the mesoporous films originates from their high porosity and ultra-high uniformity. It is noted that the absorption edges were blue-shifted by about 20 nm for all the mesoporous films. This is considered to be a quantum size effect, originating from the thin wall of the mesoporous structure.

The same synthetic strategy was also employed to control the mesophase of SiO_2 thin films. A comparably solvent-rich solution (molar composition ratio: TEOS : F127 : HCl : H_2O : EtOH = 1 : 0.006 : 0.2 : 9.2 : 30) was used as the Si-sol. First, a thin film was formed by spin-coating at 600 rpm for 5 s. Then it was aged under 60% RH for 3 days, followed by heat treatment at 400 °C. As shown in Fig. 9(a), the small-angle X-ray diffraction peaks at (100), (110), (200), (211), (220), (220), and (400) indicate the formation of the cubic mesophase. The TEM image in Fig. 9(b) shows a cubic mesoporous SiO_2 thin film formed by this slow spin-coating process. Another film was prepared by spin-coating at 2000 rpm for 20 s. After the same aging and heat treatment, a 2D hexagonal mesoporous SiO_2 film was obtained, as shown in Fig. 9(c). The X-ray diffraction pattern of calcined films only shows (*n*00) peaks, which suggests the formation of 2D hexagonal mesopores oriented parallel to the substrate. These observations on SiO_2 films again support the idea that the evaporation rate of volatile components during the spin-coating process is critical in determining the mesophases of the resultant thin films.

So far, most mesoporous TiO_2 or SiO_2 films were prepared by the dip-coating method, and only a few groups have successfully prepared mesoporous TiO_2 films with the

Downloaded by University of California - Los Angeles on 01 January 2013
Published on 05 May 2005 on http://pubs.rsc.org | doi:10.1039/B417310D

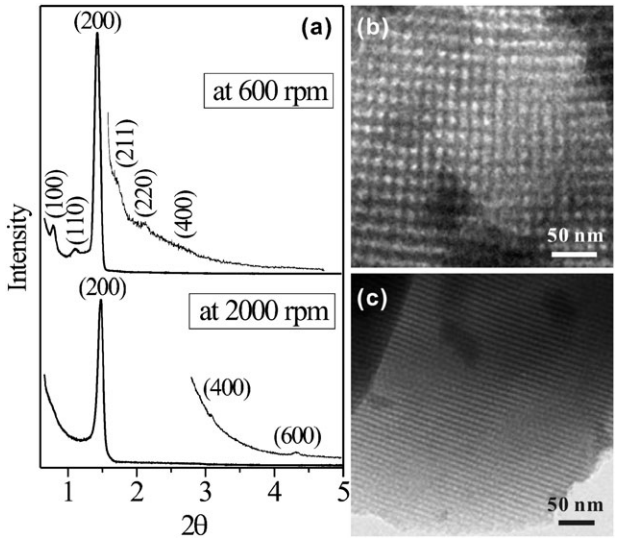

Fig. 9 (a) XRD pattern and (b, c) TEM micrographs of mesoporous SiO_2 thin films prepared by (b) spin-coating at 600 rpm for 5 s or (c) spin-coating at 2000 rpm for 20 s. Each film was calcined at 400 °C.

spin-coating process. All of the previously reported films prepared by spin-coating had the 2D-hexagonal structure.[20,22,40–43] In this work we have shown that, using the same Ti- or Si-sol, selective control of the mesoporous structure is possible by simply varying the spin-coating conditions. This process is a highly reproducible and very convenient, since the same sol solution is used to obtain either cubic or hexagonal mesophases. Generalization of this process is now being investigated in our group.

Conclusion

The mesophases of TiO_2 thin films can be selectively controlled by the speed of spin-coating *via* the EISA process. Cubic mesoporous TiO_2 thin films are obtained by dip-coating or spin-coating at a low speed, such as 600 rpm, while 2D hexagonal mesoporous TiO_2 thin films are prepared at a high spin-coating speed, for example 2000 rpm. When coating at 1000 rpm, a mixture of hexagonal and cubic mesophases is formed with no worm-like structure. It is deduced that the spinning speed influences the evaporation rate of volatile components, such as ethanol, during the spin-coating of Ti-sol, and this is critical in the determination of the mesoporous structure of the resultant TiO_2 films. This procedure is very simple and highly reproducible. The prepared mesostructure is highly ordered and the framework is so robust that the structure can be maintained up to at least 400 °C. Also, the prepared TiO_2 films show a 95% transmittance and high uniformity. This preparative concept can also be used for mesophase control of SiO_2 thin films.

Experimental

Preparation of initial sols for TiO_2 and SiO_2 thin films

Titanium tetraisopropoxide (TTIP, Aldrich) and tetraethylorthosilicate (TEOS, Aldrich) were used as the titanium and silicon sources, respectively. A triblock copolymer, Pluronic F127 (Aldrich), was used without further purification as the surfactant throughout the experiments.

For the preparation of Ti-sol, TTIP was dissolved and stabilized in an aqueous HCl solution while vigorously stirring at room temperature. After 15 min, the yellowish titania precursor solution was added to the F127 ethanol solution dropwise. The molar ratio for the synthesized Ti-sol was controlled as follows : TTIP : F127 : HCl : H_2O : EtOH = 1 : 0.005–0.0055 : 1.7–1.9 : 10–15 : 24–28.

The initial Si-sol was prepared based on the procedures reported by Zhao *et al.*[29] TEOS was heated in the mixture solution containing HCl, ethanol, and H_2O at 60 °C for 2 h. The pre-hydrolyzed solution was then added to the F127 ethanol solution dropwise. The molar ratio of the compositions in the result Si-sol was as follows: TEOS : F127 : HCl : H_2O : EtOH = 1 : 0.005–0.006 : 0.12–0.25 : 8–10 : 30–40.

Preparation of mesoporous TiO_2 and SiO_2 thin films

Both of the initial sols were aged under mild stirring conditions at room temperature for 3 h. They were then spin-coated on Pyrex glass substrates, which were pre-cleaned by the RCA method. The spinning speed and time were controlled at 600–3000 rpm and 5–20 s, respectively. For comparison, the dip-coating process was also applied for the preparation of mesoporous films. That is, after vertical immersion of the substrate for 10 s into a closed vessel containing the initial sol, it was slowly lifted up and dried in air for 3 min.

All the deposited films were aged for 3 days in a closed chamber, whose relative humidity (RH) was maintained to 60% by a saturated salt solution. The removal of F127 was carried out by heating the aged films at 350–400 °C for 4 h (ramping rate: 1 °C min^{-1}) in air.

Characterization

Small-angle X-ray diffraction patterns for the TiO_2 and SiO_2 films were obtained by using a Rigaku Multiflex diffractometer, with monochromated high-intensity Cu K_α radiation, operated at 40 kV and 20 mA. The diffraction patterns were scanned at a rate of 0.05° min^{-1} over the 2θ region of 0.6–5°. For the observation of prepared mesoporous thin films by TEM (Philips CM30 transmission electron microscope operated at 250 kV), the films were scratched off from the substrate and the collected flakes were gently dispersed in methanol. The suspension was then dropped on a holey amorphous carbon film deposited on a Ni grid (JEOL Ltd.). The optical transmissions of the TiO_2 films were recorded by an UV-visible spectrophotometer (Perkin–Elmer Lambda 40) in the wavelength range of 290–800 nm.

Acknowledgements

The authors gratefully acknowledge the financial support of the Korean Science and Engineering Foundation (KOSEF R01-2003-000-10667-0).

References

1 C. T. Kresge, M. E. Leonowicz, W. J. Roth, J. C. Vartuli and J. S. Beck, *Nature (London)*, 1992, **359**, 710.
2 J. S. Beck, J. C. Vartuli, W. J. Roth, M. E. Leonowicz, C. T. Kresge, K. D. Schmitt, C. T. W. Chu, D. H. Olson, E. W. Sheppard, S. B. McCullen, J. B. Higgins and J. L. Schlenker, *J. Am. Chem. Soc.*, 1992, **114**, 10834.
3 K. W. Gallis and C. C. Landry, *Chem. Mater.*, 1997, **9**, 2035.
4 D. Zhao, J. Feng, Q. Huo, N. Melosh, G. H. Fredrickson, B. F. Chmelka and G. D. Stucky, *Science*, 1998, **279**, 548.
5 D. Zhao, J. Feng, Q. Huo, B. F. Chmelka and G. D. Stucky, *J. Am. Chem. Soc.*, 1998, **120**, 6024.
6 J. Y. Ying, C. P. Mehnert and M. S. Wong, *Angew. Chem., Int. Ed.*, 1999, **38**, 56.
7 G. J. A. A. Soler-Illia, C. Sanchez, B. Lebeau and J. Patarin, *Chem. Rev.*, 2002, **102**, 4093.
8 G. J. A. A. Soler-Illia, E. Scolan, A. Louis, P.-A. Albouy and C. Sanchez, *New J. Chem.*, 2001, **25**, 156.
9 C. Yu, B. Tian and D. Zhao, *Curr. Opin. Solid State Mater. Sci.*, 2003, **7**, 191.
10 P. Yang, D. Zhao, D. I. Margolese, B. F. Chmelka and G. D. Stucky, *Nature (London)*, 1998, **396**, 152.
11 J. Patarin, B. Lebeau and R. Zana, *Curr. Opin. Colloid Interface Sci.*, 2002, **7**, 107.

Downloaded by University of California - Los Angeles on 01 January 2013
Published on 05 May 2005 on http://pubs.rsc.org | doi:10.1039/B417310D

View Article Online

12 G. J. A. A. Soler-Illia, E. L. Crepaldi, D. Grosso and C. Sanchez, *Curr. Opin. Colloid Interface Sci.*, 2003, **8**, 109.
13 Y. Lu, R. Ganguli, C. A. Drewien, M. T. Anderson, C. J. Brinker, W. Gong, Y. Guo, H. Soyez, B. Dunn, M. H. Huang and J. I. Zink, *Nature (London)*, 1997, **389**, 364.
14 C. J. Brinker, Y. Lu, A. Sellinger and H. Fan, *Adv. Mater.*, 1999, **11**, 579.
15 B. Alonso, A. R. Balkenende, P. A. Albouy, H. Amenitsch, M. N. Rager and F. Babonneau, *J. Sol-Gel Sci. Technol.*, 2003, **26**, 587.
16 D. Grosso, F. Babonneau, P. A. Albouy, H. Amenitsch, A. R. Balkenende, A. Brunet-Bruneau and J. Rivory, *Chem. Mater.*, 2002, **14**, 931.
17 D. Grosso, F. Cagnol, G. J. A. A. Soler-Illia, E. L. Crepaldi, H. Amenitsch, A. Brunet-Bruneau, A. Bourgeois and C. Sanchez, *Adv. Funct. Mater.*, 2004, **14**, 309.
18 J. C. Yu, X. Wang and X. Fu, *Chem. Mater.*, 2004, **16**, 1523.
19 K. L. Frindell, J. Tang, J. H. Harreld and G. D. Stucky, *Chem. Mater.*, 2004, **16**, 3524.
20 S. Y. Choi, M. Mamak, N. Coombs, N. Chopra and G. A. Ozin, *Nano Lett.*, 2004, **4**, 1231.
21 K. M. Coakley, Y. Liu, M. D. McGehee, K. L. Frindell and G. D. Stucky, *Adv. Funct. Mater.*, 2003, **13**, 301.
22 R. Vogel, P. Meredith, I. Kartini, M. Harvey, J. D. Riches, A. Bishop, N. Heckenberg, M. Trau and H. Rubinsztein-Dunlop, *ChemPhysChem*, 2003, **4**, 595.
23 M. H. Bartl, S. P. Puls, J. Tang, H. C. Lichtenegger and G. D. Stucky, *Angew. Chem., Int. Ed.*, 2004, **43**, 3037.
24 M. D. Perez, E. Otal, S. A. Bilmes, G. J. A. A. Soler-Illia, E. L. Crepaldi, D. Grosso and C. Sanchez, *Langmuir*, 2004, **20**, 6879.
25 X. Wang and J. C. Yu, *Macromol. Rapid Commun.*, 2004, **25**, 1414.
26 K. L. Frindell, M. H. Bartl, A. Popitsch and G. D. Stucky, *Angew. Chem., Int. Ed.*, 2002, **41**, 959.
27 P. C. A. Alberius, K. L. Frindell, R. C. Hayward, E. J. Kramer, G. D. Stucky and B. F. Chmelka, *Chem. Mater.*, 2002, **14**, 3284.
28 F. Bosc, A. Ayral, P.-A. Albouy, L. Datas and C. Guizard, *Chem. Mater.*, 2004, **16**, 2208.
29 D. Zhao, P. Yang, N. Melosh, J. Feng, B. F. Chmelka and G. D. Stucky, *Adv. Mater.*, 1998, **10**, 1380.
30 E. L. Crepaldi, G. J. A. A. Soler-Illia, D. Grosso and C. Sanchez, *J. Am. Chem. Soc.*, 2003, **125**, 9770.
31 D. Grosso, G. J. A. A. Soler-Illia, E. L. Crepaldi, F. Cagnol, C. Sinturel, A. Bourgeois, A. Brunet-Bruneau, H. Amenitsch, P. A. Albouy and C. Sanchez, *Chem. Mater.*, 2002, **14**, 750.
32 D. Grosso, G. J. Soler-Illia, F. Babonneau, C. Sanchez, P.-A. Albouy, A. Brunet-Bruneau and A. R. Balkenende, *Adv. Mater.*, 2001, **13**, 1085.
33 B. Smarsly, D. Grosso, T. Brezesinski, N. Pinna, C. Boissie're, M. Antonietti and C. Sanchez, *Chem. Mater.*, 2004, **16**, 2948.
34 E. L. Crepaldi, G. J. A. A. Soler-Illia, D. Grosso and C. Sanchez, *New J. Chem.*, 2003, **27**, 9.
35 E. L. Crepaldi, G. J. A. A. Soler-Illia, D. Grosso, P. A. Albouy and C. Sanchez, *Chem. Commun.*, 2001, 1582.
36 L. Pidol, D. Grosso, G. J. A. A. Soler-Illia, E. L. Crepaldi, C. Sanchez, P. A. Albouy, H. Amenitschc and P. Euzen, *J. Mater. Chem.*, 2002, **12**, 557.
37 E. L. Crepaldi, G. J. A. A. Soler-Illia, A. Bouchara, D. Grosso, D. Durand and C. Sanchez, *Angew. Chem., Int. Ed.*, 2003, **42**, 347.
38 D. Grosso, C. Boissière, B. Smarsly, T. Brezesinski, N. Pinna, P. A. Albouy, H. Amenitsch, M. Antonietti and C. Sanchez, *Nature Mater.*, 2004, **3**, 787.
39 D. O. Zarate, C. Boissiere, D. Grosso, P. A. Albouy, H. Amenitsch, P. Amoros and C. Sanchez, *New J. Chem.*, 2005, **29**, 141.
40 H. Yun, K. Miyazawa, H. Zhou, I. Honma and M. Kuwabara, *Adv. Mater.*, 2001, **13**, 1377.
41 S. Y. Choi, M. Mamak, N. Coombs, N. Chopra and G. A. Ozin, *Adv. Funct. Mater.*, 2004, **14**, 335.
42 K. S. Jang, M. G. Song, S. H. Choa and J. D. Kim, *Chem. Commun.*, 2004, 1514.
43 N. Bao, K. Yanagisawa, X. Lu and X. Feng, *Chem. Lett.*, 2004, **33**, 346.
44 A. Gibaud, D. Grosso, B. Smarsly, A. Baptiste, J. F. Bardeau, F. Babonneau, D. A. Doshi, Z. Chen, C. J. Brinker and C. Sanchez, *J. Phys. Chem. B*, 2003, **107**, 6114.

Downloaded by University of California - Los Angeles on 01 January 2013
Published on 05 May 2005 on http://pubs.rsc.org | doi:10.1039/B417310D